nuSTORM: Neutrinos from STORed Muons

Alan Bross
for the nuSTORM Collaboration

Fermi National Accelerator Laboratory, Batavia, IL 60510 USA

Abstract. The results of LSND and MiniBooNE, along with the recent papers on a possible reactor neutrino flux anomaly, give tantalizing hints of new physics. Models beyond the νSM have been developed to explain these results and involve one or more additional neutrinos that are non-interacting or "sterile." Neutrino beams produced from the decay of muons in a racetrack-like decay ring provide a powerful way to study this potential new physics. In this paper, I will describe the facility, nuSTORM, and an appropriate far detector for neutrino oscillation searches at short baseline. I will present sensitivity plots that indicated that this experimental approach can provide well over 5 σ confirmation or rejection of the LSND/MinBooNE results.

**Keywords:** sterile neutrinos, neutrino interactions, muon decay ring
PACS: 14.60.Pq, 25.30.Pt

OVERVIEW

The idea of using a muon storage ring to produce a high-energy ($\simeq 50$ GeV) neutrino beam for experiments was first discussed by Koshkarev [1] in 1974. A detailed description of a muon storage ring for neutrino oscillation experiments was first produced by Neuffer [2] in 1980. In his paper, Neuffer studied muon decay rings with E_μ of 8, 4.5 and 1.5 GeV. With his 4.5 GeV ring design, he achieved a figure of merit of $\simeq 6 \times 10^9$ useful neutrinos per 3×10^{13} protons on target. The facility we describe here (nuSTORM) is essentially the same facility proposed in 1980 and would utilize a $\simeq 4$ GeV/c muon storage ring to study eV-scale oscillation physics and, in addition, could add significantly to our understanding of ν_e and ν_μ cross sections. In particular the facility can:

1. address the large Δm^2 oscillation regime and make a major contribution to the study of sterile neutrinos,
2. make precision ν_e and $\bar{\nu}_e$ cross-section measurements and greatly expand our undertanding of ν interaction physics in general,
3. provide an accelerator technology test facility that will be able to test instrumenation in the decay ring and can provide a low-energy intense μ beam for future 6D muon ionization cooling studies,
4. provide a precisely understood ν beam for detector studies.

The facility is the simplest implementation of the Neutrino Factory concept [3]. In our case, 60-120 GeV/c protons are used to produce pions off a conventional solid target. The pions are collected with a focusing device (horn) and are then transported to, and injected into, a storage ring. The pions that decay in the first straight of the ring can yield a muon that is captured in the ring. The circulating muons then subsequently decay into electrons and neutrinos. We are starting with a storage ring design that is optimized for 3.8 GeV/c muon momentum. This momentum was selected to maximize the physics reach for both oscillation and the cross section physics. See Fig. 1 for a schematic of the facility.
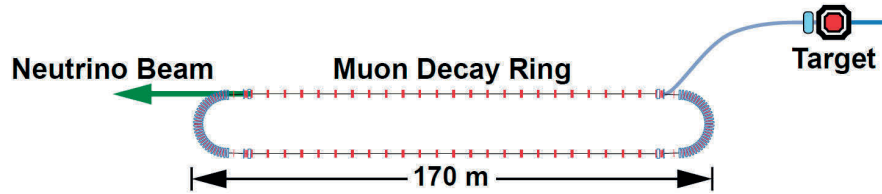
Figure 1. Schematic of the facility

Muon decay yields a neutrino beam of precisely known flavor content and energy spectrum. For example for positive muons: $\mu^+ \to e^+ + \bar{\nu}_\mu + \nu_e$. In addition, if the circulating muon flux in the ring is measured accurately (with beam-current transformers, for example), then the neutrino beam flux is also accurately known. Near and far detectors are placed along the line of one of the straight sections of the racetrack decay ring. The near detector can be placed at 50 meters from the end of the straight. A near detector for disappearance measurements will be identical to the far detector, but only about one tenth the fiducial mass. It will require a μ catcher, however. Additional purpose-specific near detectors can also be located in the near hall and will measure neutrino-nucleon cross sections. nuSTORM can provide the first precision measurements of ν_e and $\bar{\nu}_e$ cross sections which are important for future long-baseline experiments. A far detector at $\simeq 2000$ m would study neutrino oscillation physics and would be capable of performing searches in both appearance and disappearance channels. The experiment will take advantage of the "golden channel" of oscillation appearance $\nu_e \to \nu_\mu$, where the resulting final state has a muon of the wrong-sign from interactions of the $\bar{\nu}_\mu$ in the beam. In the case of μ^+s stored in the ring, this would mean the observation of an event with a μ^-. This detector would need to be magnetized for the wrong-sign muon appearance channel, as is the case for the current baseline Neutrino Factory detector [4]. A number of possibilities for the far detector exist. However, a magnetized iron detector similar to that used in MINOS is likely to be the most straight forward approach for the far detector design. We believe that it will meet the performance requirements needed to reach our physics goals. For the purposes of the nuSTORM oscillation physics, a detector inspired by MINOS, but with thinner plates and much larger excitation current (larger B field) is assumed.

THEORETICAL AND EXPERIMENTAL MOTIVATIONS

Sterile neutrinos in extensions of the Standard Model

Sterile neutrinos, fermions that are uncharged under the $SU(3) \times SU(2) \times U(1)$ gauge group, arise naturally in many extensions to the Standard Model. Even where they are not an integral part of a model, they can usually be easily accommodated. A detailed overview of the phenomenology of sterile neutrinos and of related model building considerations is given in [5].

Models attempting to explain the smallness of neutrino masses through a seesaw mechanism generically contain sterile neutrinos. While in the most generic seesaw scenarios, these sterile neutrinos are extremely heavy ($\sim 10^{14}$ GeV) and have very small mixing angles ($\sim 10^{-12}$) with the active neutrinos, slightly non-minimal seesaw models can easily feature sterile neutrinos with eV-scale masses and with percent level mixing with the active neutrinos. Examples for non-minimal seesaw models with relatively light sterile neutrinos include the split seesaw scenario [6], seesaw models with additional flavor symmetries (see e.g. [7]), models with a Froggatt-Nielsen mechanism [8, 9], and extended seesaw models that augment the mechanism by introducing more than three singlet fermions, as well as additional symmetries [10, 11, 12].

While the theoretical motivation for the existence of sterile neutrinos is certainly strong, what has mostly prompted the interest of the scientific community in this topic are several experimental results that show significant deviations from the Standard Model predictions. These results can be interpreted as hints for oscillations involving sterile neutrinos.

The first of these hints was obtained by the LSND collaboration, who carried out a search for $\bar{\nu}_\mu \to \bar{\nu}_e$ oscillations over a baseline of ~ 30 m [13]. Neutrinos were produced in a stopped pion source in the decay $\pi^+ \to \mu^+ + \nu_\mu$ and the subsequent decay $\mu^+ \to e^+ \bar{\nu}_\mu \nu_e$. Electron antineutrinos are detected through the inverse beta decay reaction $\bar{\nu}_e p \to e^+ n$ in a liquid scintillator detector. Backgrounds to this search arise from the decay chain $\pi^- \to \bar{\nu}_\mu + (\mu^- \to \nu_\mu \bar{\nu}_e e^-)$ if negative pions produced in the target decay before they are captured by a nucleus, and from the reaction $\bar{\nu}_\mu p \to \mu^+ n$, which is only allowed for the small fraction of muon antineutrinos produced by pion decay *in flight* rather than stopped pion decay. The LSND collaboration finds an excess of $\bar{\nu}_e$ candidate events above this background with a significance of more than 3σ. When interpreted as $\bar{\nu}_\mu \to \bar{\nu}_e$ oscillations through an intermediate sterile state $\bar{\nu}_s$, this result is best explained by sterile neutrinos with an effective mass squared splitting $\Delta m^2 \gtrsim 0.2$ eV^2 relative to the active neutrinos, and with an effective sterile-induced $\bar{\nu}_\mu$–$\bar{\nu}_e$ mixing angle $\sin^2 2\theta_{e\mu,\text{eff}} \gtrsim 2 \times 10^{-3}$, depending on Δm^2.

The MiniBooNE experiment [14, 15] was designed to test the neutrino oscillation interpretation of the LSND result using a different technique, namely neutrinos from a horn-focused pion beam. While a MiniBooNE search for $\nu_\mu \to \nu_e$ oscillations indeed disfavors most (but not all) of the parameter region preferred by LSND in the simplest model with only one sterile neutrino [14], the experiment obtains results *consistent* with LSND when running in antineutrino mode

and searching for $\bar{\nu}_\mu \to \bar{\nu}_e$. Due to low statistics, however, the antineutrino data favors LSND-like oscillations over the null hypothesis only at the 90% confidence level. Moreover, MiniBooNE observes a yet unexplained 3.0σ excess of ν_e-like events (and, with smaller significance also of $\bar{\nu}_e$ events) at low energies, 200 MeV $\lesssim E_\nu \lesssim$ 475 MeV, outside the energy range where LSND-like oscillations would be expected.

A third hint for the possible existence of sterile neutrinos is provided by the so-called reactor antineutrino anomaly. In 2011, Mueller *et al.* published a new *ab initio* computation of the expected neutrino fluxes from nuclear reactors [16]. Their results improve upon a 1985 calculation by Schreckenbach [17] by using up-to-date nuclear databases, a careful treatment of systematic uncertainties and various other corrections and improvements that were neglected in the earlier calculation. Mueller *et al.* find that the predicted antineutrino flux from a nuclear reactor is about 3% higher than previously thought. This result, which was later confirmed by Huber [18], implies that short baseline reactor experiments have observed a 3σ *deficit* of antineutrinos compared to the prediction [19, 5]. It needs to be emphasized that the significance of the deficit depends crucially on the systematic uncertainties associated with the theoretical prediction, some of which are difficult to estimate reliably. If the reactor antineutrino deficit is interpreted as $\bar{\nu}_e \to \bar{\nu}_s$ disappearance via oscillation, the required 2-flavor oscillation parameters are $\Delta m^2 \gtrsim 1$ eV^2 and $\sin^2 2\theta_{ee,\text{eff}} \sim 0.1$.

Such short-baseline oscillations could also explain another experimental result: the Gallium anomaly. The GALLEX and SAGE solar neutrino experiments used electron neutrinos from intense artificial radioactive sources to test their radiochemical detection principle [20, 21, 22, 23, 24]. Both experiments observed fewer ν_e from the source than expected. The statistical significance of the deficit is above 99% and can be interpreted in terms of short-baseline $\bar{\nu}_e \to \bar{\nu}_s$ disappearance with $\Delta m^2 \gtrsim 1$ eV^2 and $\sin^2 2\theta_{ee,\text{eff}} \sim$ 0.1–0.8. [25, 26, 27].

A number of recent articles have presented detailed reviews of the status of neutrino-nucleon scattering cross section measurements in the context of the oscillation-physics program (see for example [28] and references therein). The effect of uncertainties in the neutrino scattering cross sections is to reduce the sensitivity of the present and future short- and long-baseline experiments and the impact of the uncertainties on the cross sections is particularly pernicious at large θ_{13}. The neutrino flux that will be generated by the 3.8 GeV stored muon beam proposed here will allow cross section measurements in the neutrino-energy range $1 - 3$ GeV, the region in which the $\nu_\mu N$ data is sparse. Moreover, ν_e appearance searches rely on $\nu_e N$ cross sections for which there is essentially no data. At present, estimates of the electron-neutrino cross sections are made by extrapolation of the muon neutrino cross sections. Such extrapolations suffer from substantial uncertainties arising from non-perturbative hadronic corrections and it is therefore essential that detailed measurements of the $\nu_e N$ and $\nu_\mu N$ scattering cross sections and hadron-production rates are performed. The nuSTORM facility, therefore, has a unique opportunity. The flavor composition of the beam and the neutrino energy spectrum are both known precisely. In addition, the storage ring instrumentation combined with measurements at the near detector will allow the neutrino flux to be measured with a precision of 1%. Substantial event rates may be obtained in a fine-grained detector placed between 20 m and 50 m from the storage ring. Therefore, the objective is to measure the $\nu_e N$ and $\nu_\mu N$ scattering cross sections for neutrino energies in the range $1 - 3$ GeV with a precision approaching 1%. This will be a critical contribution to the search for sterile neutrinos and will be of fundamental importance to the present and next generation of long-baseline neutrino oscillation experiments.

FACILITY

The basic concept for the facility is presented in Fig. 1. A high-intensity proton source places beam on a target, producing a large spectrum of secondary pions. Forward pions are focused by a horn into a transport channel. Pions decay within the first straight of the decay ring and a fraction of the resulting muons are stored in the ring. Muon decay within the straight sections will produce ν beams of known flux and flavor via: $\mu^+ \to e^+ + \bar{\nu}_\mu + \nu_e$ or $\mu^- \to e^- + \nu_\mu + \bar{\nu}_e$. For the implementation which is described here, we choose a 3.8 GeV/c storage ring to obtain the desired spectrum of $\simeq$ 2-3 GeV neutrinos. This means that we must capture pions at a momentum of approximately 5 GeV/c.

The number of pions produced off various targets by 60 GeV/c protons has been simulated with the MARS code [29]. The results of this analysis on a number of different targets yielded the pion rate in a foward cone of 120 mrad, per proton on target. A target optimization based on a conservative estimate for the decay-ring acceptance of 2 mm-radian was then done which indicated a yield of approximately 0.10 π^+/POT can be collected into a $\pm$ 10% momentum acceptance off medium/heavy targets assuming 80% capture efficiency.

An obvious goal for the facility is to collect as many pions as possible (within the limits of available beam power), inject them into the decay ring and capture as many muons as possible from the $\pi \to \mu$ decays. With pion decay within the ring, non-Liouvillean "stochastic injection" is possible. In stochastic injection, the $\simeq$ 5 GeV/c pion beam is transported from the target into the storage ring and dispersion-matched into a long straight section. (Circulating and

injection orbits are separated by momentum.) Decays within that straight section provide muons that are within the $\simeq 3.8$ GeV/c ring momentum acceptance see Fig. 2. Note: for 5.0 GeV/c pions, the decay length is $\simeq 280$m; $\simeq 42\%$ decay within the 150m decay ring straight.
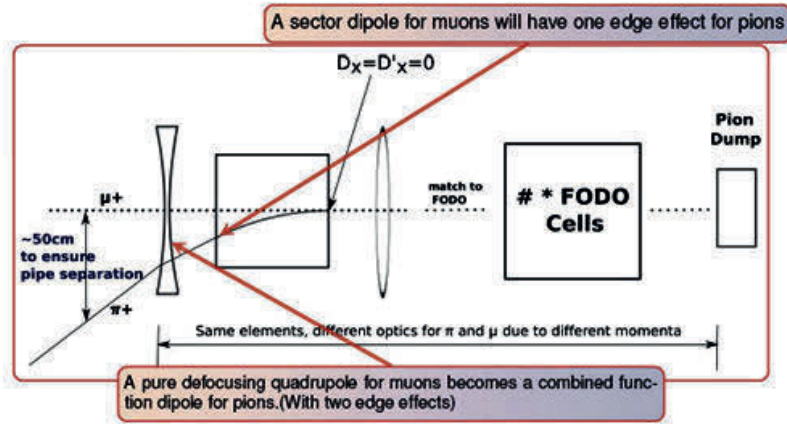

Figure 2. Stochastic injection concept

The baseline for the muon decay ring is a FODO racetrack, although a FFAG racetrack is also being investigated. The FODO ring uses both normal and superconducting magnets. A FODO lattice using only normal-conducting magnets ($B \lesssim 2T$) is also being developed. In this case, the arcs are twice as long ($\simeq 50$m), but the straight sections would be similar. The design goal for the ring was to maximize both the transverse and momentum acceptance (around 3.8 GeV/c central momentum), while maintaining reasonable physical apertures for the magnets in order to keep the cost down. This was accomplished by employing strongly focusing optics in the arcs (90 deg. phase advance per cell FODO); featuring small β functions ($\simeq 3$ m average) and low dispersion ($\simeq 0.8$ m average).
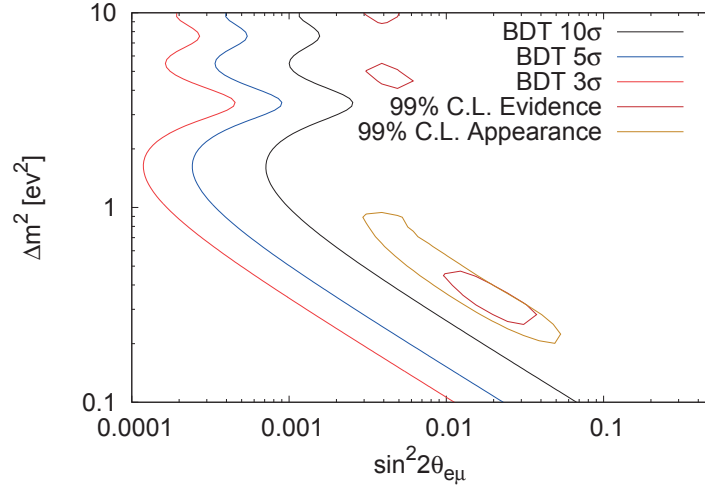

FAR DETECTOR - SUPERBIND

The Super-B Iron Neutrino Detector (SuperBIND) is an iron and scintillator sampling calorimeter which is similar in concept to the MINOS detectors [30]. We have chosen a cross section of approximately 5 m in order to maximize the ratio of the fiducial mass to total mass. The magnetic field will be toroidal as in MINOS and SuperBIND will also use extruded scintillator for the readout planes.

SIMULATION AND ANALYSIS FOR A ν_μ APPEARANCE SEARCH

A detailed simulation of the SuperBIND detector has been developed, based on the Neutrino Factory Magnetised Iron Neutrino Detector (MIND) [31], to determine the sensitivity of the nuSTORM facility to LSND-like anomalies in short baseline oscillation experiments. The GENIE event generator[32] is used to simulate neutrino interactions with the detector material, while GEANT4[33] is used to propagate the products of the interactions through the detector volume. The geometry is defined locally within the GEANT4 framework in a flexible way to allow for optimization of the detector geometry — for example altering the dimensions of the detector and the depth of individual iron or scintillator planes. For the purpose of the simulated results shown here a 20 m long detector with a cylindrical cross-section 2.5 m was assumed, with 2 cm iron plates providing the magnetic field between 2 cm of scintillator material. Hadron interactions are included in the simulation through the usage of the QGSP_BERT physics lists[33]. Particle hits in the scintillator bars are grouped into clusters, smeared in position, and the accumulated energy loss is attenuated by the propagation distance using a simple digitization algorithm applied prior to reconstruction.

The reconstruction uses multiple passes of a Kalman filtering and fitting algorithm for the purposes of identifying muon trajectories within events and to determine the momentum and charge for an identified track. These fitting algorithms are supplied by use of the RecPack software package[34]. Geometric information such as the extent and initial pitch of the track is used to provide initial estimates for the algorithm to progress the fit through the provided space points. The hadron reconstruction is not yet well developed so the neutrino energy is reconstructed either by the

Figure 3. The 3σ, 5σ, and 10σ sensitivity contours for the SuperBIND detector at νSTORM shown with 99% confidence levels from existing neutrino oscillation appearance data.

quasi-elastic approximation if no data points attributable to hadronization are visible, or by smearing the true hadron energy according to the results of the MINOS CalDet test beam[30]. However, the analysis does fit for multiple tracks within an event. The muon track in a given event is defined by the longest trajectory fit in the event.

The muon reconstruction is subjected to a further analysis routine to select events with a well identified muon rather than those where muons are mis-identified either in charge or identity. To achieve the target of 10σ significance, the background efficiency must be reduced to less than 1 part in 10^4. The selection of events is accomplished with a multivariate analysis facilitated by the root based TMVA package. This analysis outperforms the previously described cuts based analysis[35] by offering a lower energy signal threshold which increases the sensitivity of the experiment to oscillations.

The analysis was trained to discriminate between ν_μ charge current (CC) interactions signal events and $\bar{\nu}_\mu$ neutral current (NC) interaction background events using a suite of five parameters to define a classifier. The majority of these parameters were chosen based on the experience of the MINOS experiment [36].

The appearance channel $\nu_e \to \nu_\mu$ is broadly sensitive to sterile neutrinos and allows nuSTORM to test the LSND/MiniBooNe anomaly. This analysis focusses on the appearance signal $\nu_e \to \nu_\mu$ which is the CPT conjugate of the $\bar{\nu}_\mu \to \bar{\nu}_e$ appearance channel of the observed LSND anomaly. The strong suppression of background possible at nuSTORM using a wrong sign muon search means that the experiment will be very sensitive to the appearance channel.

The trained BDT analysis is applied to the simulations to extract the detector response for the purpose of a full determination of the experimental sensitivity to oscillation parameters assuming the existence of sterile neutrinos. The detector response is formatted as a "migration matrix" consisting of probabilities that a neutrino generated in an energy bin, i, should be reconstructed in the jth energy bin. Thus the migration matrix contains information for both the energy resolution and response. The GloBES software package is used to simulate the neutrino flux generated by the storage ring propagated over the two kilometre baseline assuming a 3+1 neutrino model. The signal response from ν_μ CC events is used with the background response to $\bar{\nu}_\mu$ CC, $\bar{\nu}_\mu$ NC, ν_e CC, and ν_e NC events to determine the number of events detected after oscillation.

The (statistics only) sensitivity to oscillations in nuSTORM, based on 2×10^{18} useful μ decays for an exposure of 10^{21} protons on target, as a function of the mass squared difference Δm^2_{41}, and the effective mixing angle $\sin^2 2\theta_{e\mu} = |U_{e4}|^2 |U_{\mu\,4}|^2$ is shown in Fig. 3. Contours showing the 99% confidence levels for the combination of LSND, MiniBooNE, Gallex, and existing reactor experiments are shown, as well as the 99% confidence level when data from all compatible appearance experiments, including KARMEN, NOMAD, and ICARUS are added to the fit. The muon neutrino appearance channel at nuSTORM can make a measurement surpassing 10σ significance over the entire phase space consistent with the LSND anomaly, and can conclusively determine the existence or non-existence of sterile neutrinos.

REFERENCES

1. D. G. Koshkarev, Proposal for a Decay Ring to Produce Intense Secondary Particle Beams at the SPS (1974), CERN/ISR-DI/74-62.
2. D. Neuffer, Design Considerations for a Muon Storage Ring (1980), Telmark Conference on Neutrino Mass, Barger and Cline eds., Telmark, Wisconsin.
3. S. Geer, *Phys.Rev.* **D57**, 6989–6997 (1998).
4. S. Choubey, et al. (2011).
5. K. Abazajian, M. Acero, S. Agarwalla, A. Aguilar-Arevalo, C. Albright, et al. (2012).
6. A. Kusenko, F. Takahashi, and T. T. Yanagida, *Phys.Lett.* **B693**, 144–148 (2010).
7. R. Mohapatra, *Phys.Rev.* **D64**, 091301 (2001).
8. C. Froggatt, and H. B. Nielsen, *Nucl.Phys.* **B147**, 277 (1979).
9. J. Barry, W. Rodejohann, and H. Zhang, *JCAP* **1201**, 052 (2012).
10. R. Mohapatra, S. Nasri, and H.-B. Yu, *Phys.Rev.* **D72**, 033007 (2005).
11. C. S. Fong, R. N. Mohapatra, and I. Sung, *Phys.Lett.* **B704**, 171–178 (2011).
12. H. Zhang (2011).
13. A. Aguilar, et al., *Phys. Rev.* **D64**, 112007 (2001).
14. A. Aguilar-Arevalo, et al., *Phys.Rev.Lett.* **98**, 231801 (2007).
15. A. Aguilar-Arevalo, et al., *Phys.Rev.Lett.* **105**, 181801 (2010).
16. T. Mueller, D. Lhuillier, M. Fallot, A. Letourneau, S. Cormon, et al., *Phys.Rev.* **C83**, 054615 (2011).
17. K. Schreckenbach, G. Colvin, W. Gelletly, and F. Von Feilitzsch, *Phys.Lett.* **B160**, 325–330 (1985).
18. P. Huber, *Phys.Rev.* **C84**, 024617 (2011).
19. G. Mention, M. Fechner, T. Lasserre, T. Mueller, D. Lhuillier, et al., *Phys.Rev.* **D83**, 073006 (2011).
20. P. Anselmann, et al., *Phys.Lett.* **B342**, 440–450 (1995).
21. W. Hampel, et al., *Phys.Lett.* **B420**, 114–126 (1998).
22. J. Abdurashitov, V. Gavrin, S. Girin, V. Gorbachev, T. V. Ibragimova, et al., *Phys.Rev.Lett.* **77**, 4708–4711 (1996).
23. J. Abdurashitov, et al., *Phys.Rev.* **C59**, 2246–2263 (1999).
24. J. Abdurashitov, V. Gavrin, S. Girin, V. Gorbachev, P. Gurkina, et al. .
25. M. A. Acero, C. Giunti, and M. Laveder, *Phys.Rev.* **D78**, 073009 (2008).
26. C. Giunti, and M. Laveder, *Phys.Rev.* **D82**, 053005 (2010).
27. C. Giunti, and M. Laveder, *Phys.Rev.* **C83**, 065504 (2011).
28. J. Hewett, H. Weerts, R. Brock, J. Butler, B. Casey, et al. (2012).
29. N. Mokhov, V. Pronskikh, I. Rakhno, S. Striganov, I. Tropin, et al. (2012).
30. D. G. Michael, et al., *Nucl. Instrum. Meth.* **A596**, 190–228 (2008).
31. R. Bayes, A. Laing, F. Soler, A. C. Villanueva, J. G. Cadenas, et al., *Phys. Rev. D* **86**, 093015 (2012), URL http://link.aps.org/doi/10.1103/PhysRevD.86.093015.
32. C. Andreopoulos, et al., *Nucl. Instrum. Meth. A* **614**, 87–104 (2010).
33. J. Apostolakis, and D. H. Wright, *AIP Conf. Proc.* **896**, 1–10 (2007).
34. A. Cervera-Villanueva, J. J. Gomez-Cadenas, and J. A. Hernando, *Nucl. Instrum. Meth.* **A534**, 180–183 (2004).
35. P. Kyberd, et al. (2012).
36. P. Adamson, et al., *Phys. Rev. D* **82**, 051102 (2010).